ChemistrySelect

Research Article
doi.org/10.1002/slct.202404218

Chemistry Europe
European Chemical Societies Publishing

www.chemistryselect.org

Synthesis of Aluminum Complexes Based on 2,6-Bis(2-hydroxyphenyl)Pyridines: Efficient Initiators for Ring-Opening Polymerization of Cyclic Esters

Valeriia A. Serova,[a, b] Artem V. Lykov,[a, b] Badma N. Mankaev,[a, b] Milana U. Agaeva,[a, b] Konstantin A. Lyssenko,[a] Elena V. Chernikova,[a] Maxim V. Zabalov,[b, c] Mikhail P. Egorov,[b] and Sergey S. Karlov*[a, b]

The search for new initiators based on nontoxic metal complexes, allowing for the controlled production of polycaprolactone (PCL) and polylactide (PLA) is an actual task. In the present work, we report the synthesis of aluminum complexes **6a** and **6b** based on substituted 2,6-bis(2-hydroxyphenyl)pyridine proligands. The compositions and structures of the novel compounds were established by elemental analysis and ^{1}H, ^{13}C, NMR spectroscopy in the solid state by X-ray diffraction analysis (**6a and 6b**). All the synthesized aluminum complexes are monomeric. Complexes **6a** and **6b** (in presence of benzyl alcohol (BnOH)) turned out to be active in the ring opening polymerization (ROP) of ε-caprolactone (ε-CL), L-, *rac*-lactide (L-, *rac*-LA) gave PCL and PLA with high molecular weights. The mechanism of the polymerization reaction for compounds **C**, **6a,** and **6b** was also investigated using the density functional theory (DFT) method. The substituent effect analyzed in terms of percent buried volume and non-covalent interactions. The values of calculated Gibbs free activation energies correspond to the trend found experimentally.

1. Introduction

Nowadays, the problem of environmental pollution is acute. In particular, with the accumulation of traditional polyolefin plastics, which are almost nondegradable in the world's oceans and in the Earth's soil. Accordingly, biodegradable polymers are designed to solve some of these problems. The main method of obtaining biodegradable polymers such as PCL, PLA, and others is ROP of cyclic esters. This process requires the presence of a metal catalyst, stannous octoate ($Sn(Oct)_2$) in the presence of alcohol is preferred to be used in industry because of its stability and significant activity at high temperatures. However, the required high temperatures contribute to the occurrence of side undesirable processes, such as transesterification. The debate about the toxicity of tin does not end,[1] but it's believed that the accumulation of tin in the human body is presumably harmful. The use of polymers obtained by this way in medicine as pins or suture material or in food industry as packaging material requires careful purification of the polymer from traces of the initiator. In connection with increasing requirements for biomedical materials, the development of new initiators based on non-toxic metals, allowing the production of biodegradable polymers, such as PCL and PLA, in a controlled manner, with the required molecular weights and molecular weight distribution, remains relevant.[2] It is also very important to study series of closely related initiators that differ in the nature of the substituents in the molecule in order to find factors that affect the activity of the initiator and other reaction parameters.

Studies of aluminum complexes in ROP are the most numerous due to their low cost and low toxicity of this element.[3] Recently, interest has grown in aluminum complexes with a coordination number (CN) of aluminum of 5, one of which are aluminum complexes based on salen-type ligands (Type A, Figure 1), due to their ability to cause stereoregular polymerization of *rac*-LA.[4] However, aluminum complexes with 4-coordinated aluminum are more active than with 5-coordinated aluminum due to the greater availability of the metal atom for attacking the monomer. Among the initiators with 4-coordinated aluminum, complexes based on amino-bisphenol type ligands (Type B, Figure 1) are more widely used.[5]

The mechanism of ROP has been studied intensively by methods of quantum chemistry[6] and continues to be researched at present time.[7] Most of the previous studies consider the coordination-insertion mechanism as the main one.[6,7b,d,8] We especially note recent publications related to the computational study of ROP by catalysis of aluminum complexes.

[a] *V. A. Serova, A. V. Lykov, Dr. B. N. Mankaev, M. U. Agaeva, Dr. K. A. Lyssenko, Dr. E. V. Chernikova, Prof. Dr. S. S. Karlov*
Chemistry Department, Moscow State University, B-234 Leninskie Gory, Moscow 119991, Russian Federation
E-mail: s.s.karlov@chemistry.msu.ru

[b] *V. A. Serova, A. V. Lykov, Dr. B. N. Mankaev, M. U. Agaeva, Dr. M. V. Zabalov, Prof. Dr. M. P. Egorov, Prof. Dr. S. S. Karlov*
N. D. Zelinsky Institute of Organic Chemistry, Russian Academy of Sciences, Leninsky Prospect 47, Moscow 119991, Russian Federation

[c] *Dr. M. V. Zabalov*
N. N. Semenov Federal Research Center for Chemical Physics Russian Academy of Sciences, Kosygina Street 4, Moscow 119991, Russian Federation

Supporting information for this article is available on the WWW under https://doi.org/10.1002/10.1002/slct.202404218

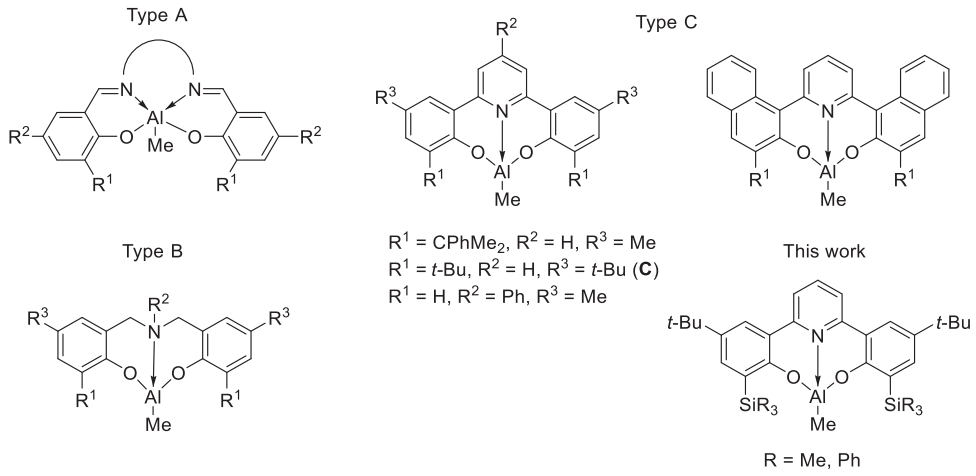

Figure 1. Aluminum complexes in ROP.

Chandanabodhi and Nanok studied the mechanism of copolymerization of LA and CL initiated by complexes of aluminum alkoxide with salen-type ligands.[8b] The results show that the activation barriers for the rate-determining states depend on the initiator structure. The reactivities of the initiators toward the ROP of LA and CL depend on type of bridging units and electronic properties of the ligand substituents. Nifant'ev et al. studied the copolymerization of LA and CL catalyzed by complexes of magnesium, aluminum, and zinc with 2,6-di-*t*-butyl-4-methylphenyloxy substituents.[8c,d] Authors emphasize that the formation of a highly stable chelate product of LA ring opening is a key control factor of the process.

Recently, Wongnongwa et al. studied a mechanism of homo- and co-polymerization of LA and CL catalyzed by an aluminum complexes bearing a *bis*(phenoxy)amine ligand with pyridine and diethylamine sidearms.[8h] These authors found that depending on amine sidearm and the extent of noncovalent interactions of monomers with catalysts the tapered or random products can form during the co-polymerization process.

Mandal et al. using framework distortion energy (FDE) model and Gibbs free activation energy calculation by DFT method showed that modification of ligand side arm and addition electron withdrawing groups in aluminum complex with a bis-indolide Schiff-base ligand distort structure of initiator and that generally promotes effective catalysis of ROP.[9]

D'Alterio et al. found the stereoselective preference for D and L-LA polymerization depending on active site reorganization and structure of catalytic pocket of salen-Al complexes.[7b] Rusconi at al. investigated the mechanism of *poly*(lactic-co-glycolic acid) formation catalyzed by enantiopure SalBinap–Al complex. The alternating behavior of the two monomers was rationalized by unveiling the active site fluxionality of the enantiopure catalyst, identifying the rate-limiting steps that encode a preference at the glycolyl site versus the lactyl site, and revealing selection of the opposite monomer enantioface.[7c] The same authors also investigated mechanism of stereoselective *rac*-LA ROP promoted by enantiopure Salen catalysts with different metal atom (Al, Sc, Y, La). They found that Gibbs free activation energies depend on ligand wrapping modes and monomer enantiofaces in transition states. Increasing the size of the catalytic pocket relaxes the catalytic structure, allowing access to both enantiomers, inevitably leading to a loss of stereoselectivity, but to increase in catalytic activity of initiator.[7d]

We also investigated the mechanism of co-polymerization of LA and CL using aluminum and gallium amino-*bis*(phenolates) as an initiators[8f,g] and found that The stability of the chelate intermediate forming after LA insertion to the polymer chain plays a key role in the kinetics of the homo- and co-polymerization of LA and result in block co-polymer formation.

Our development of the aminobisphenol-type of ligands led to complexes based on pyridinebisphenol ligands (Type C, Figure 1).[10] These ligands are more rigid than aminobisphenols and they are a kind of balance between salen and aminobisphenol type of ligands. We have previously established that complex **C** (Figure 1, Type C, $R^1 = R^2 = R^3 = R4 =$ *t*-Bu) demonstrated excellent efficiency in the presence of one equivalent of BnOH as an external nucleophile in obtaining both PCL and PLA homopolymers and their copolymer containing monomer units in a 1:1 ratio.[10c]

Thus, to continue our previous work,[10c] it was decided to synthesize new closely related ligands with the possibility to vary the steric volume of substituents in the immediate vicinity of the metal atom, synthesize aluminum complexes based on these ligands and study their catalytic activity during polymerization. The focus of our study was on compounds containing Me_3Si and Ph_3Si groups in *ortho*-positions to the phenolate oxygen atoms, as well as a comparison of their behavior with that of the previously studied *t*-Bu derivative **C**. A possible change in the size of the substituents could change the activity of the initiators and also affect the stereochemical result of the polymerization.

In addition, the mechanism and the substituent effect in the catalyst were rationalized by using the DFT calculation. The influence of noncovalent interactions (NCI) on steric volume of catalytic pocket was analyzed. Gibbs free energy surfaces of initiation stage of ROP of ε-CL indicated that the bulkiness of substituents near the metal center increases the activation barrier of the polymerization reaction.

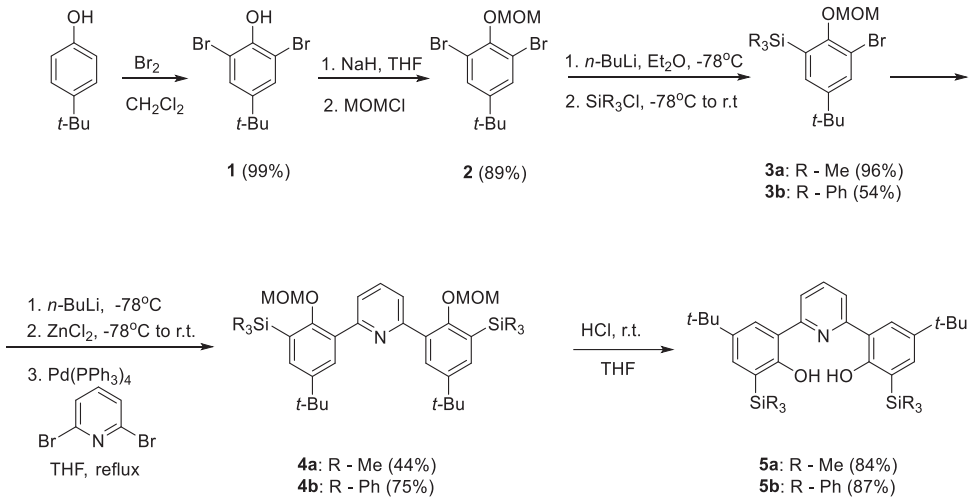

Scheme 1. Synthesis of ONO-ligands **5a** and **5b**.

2. Results and Discussion

2.1. Synthesis of ONO-Ligands

A convenient method for the synthesis of pyridine–diphenol ligands is the Negishi cross-coupling reaction. This makes it possible to obtain related ligands with different substituents starting from phenols.

Standard bromination and MOM-protection reactions were carried out with p-*t*-butylphenol (Scheme 1). Next, the introduction of a silicon-containing group (silylation reaction) was carried out. During this reaction, it is possible to use various chlorosilanes, which led to obtain ligands with different steric volume. When conducting the Negishi reaction, great attention should be paid to the choice of the ratio of reagents. Then the MOM-protection was removed. The removal of the protection group must be carried out under mild conditions to prevent the severing of the C—Si connection and the removal of the SiR_3 group. The using of standard MOM-protection (treatment of solutions **4a** and **4b** in methanol with concentrated HCl upon heating) removal method[11] led to the formation of pyridine–bisphenol without silyl groups. The other procedure[4g] was optimized (treatment of a solution of **4a** and **4b** in THF with concentrated HCl at room temperature): compounds with different substituents require different reaction times. With less time of reaction, complete removal of the protection is not observed, but with longer time, the rupture of C—Si bonds (in *ortho*-positions to the phenolate oxygen atoms) is observed. As a result, new ligands **5a** and **5b** were obtained with good yields at each stage.

2.2. Synthesis of Aluminum Complexes

The reaction of toluene solutions of the pyridine−bisphenol ligands **5a** (R = Me) and **5b** (R = Ph) with 1.1 equiv. of $AlMe_3$ in toluene at −33 °C afforded selectively the corresponding Al(III) methyl complexes **6a** and **6b**, which were isolated as yellowish solids with good yields (87% and 73%, respectively) (Figure 3). The solubility of compound **6b** in aromatic hydrocarbons (benzene, toluene) is significantly lower compared to compound **6a**. Compounds **6a, 6b** were characterized in solution by NMR spectroscopy and in the solid state by a single crystal X-ray diffraction study for **6a**.

The ^1H and ^{13}C NMR spectra of **6a, 6b** in $CDCl_3$ solution show that both complexes are monomeric in solutions. In particular, the pyridine hydrogens appear as a triplet (δ 8.03 and δ 7.83 respectively for **6a** and **6b**) and Al-CH_3 hydrogens as a singlet (δ −0.96 and δ −1.71 respectively) (Scheme 2).

The molecular structures of **6a** and **6b** (Figure 2) features an Al atom four-coordinated by the tridentate ligand and the methyl group in a distorted trigonal monopyramidal geometry (τ = 0.895 and 0.875)[12] (angles around Al 96.2(1)−117.2(2)° and 95,4)). The Al—O bond lengths in **6a and 6b** are similar (1.740(3) – 1.755(4) Å) and compare well with those observed for related Al bis(phenolate) complexes (1.7445(14)−1.7588(14) Å).[6b,6c] The Al←N bonds are by 0.1 and 0.05 Å shorter than its known for related Al aminobis(phenolate) complexes (2.01 Å for Al←N.[5a] It should be noted that some shortening of the length of the Al—N bond in **6a** and **6b** in comparison with the aminobis(phenolate) complexes is apparently associated with a more rigid structure of the pyridine-containing ligand.

We also investigated the stability of synthesized ONO-type aluminum complexes in air and with increasing temperature. The ^1H NMR spectrum of complex compound **6a**, which was exposed to air for two hours, does not differ from the spectrum of a freshly prepared compound. For compound **6b**, data were obtained by differential scanning calorimetry (DSC) and thermogravimetry (TG) (Supporting Information, Figure S17). The initial mass loss, which amounted to 10.52%, is explained by toluene residues in the aluminum complex sample. As can be seen, the synthesized complex **6b** is thermally stable up to 300 °C, which makes it possible to use the resulting complex in polymerizations at high temperatures.

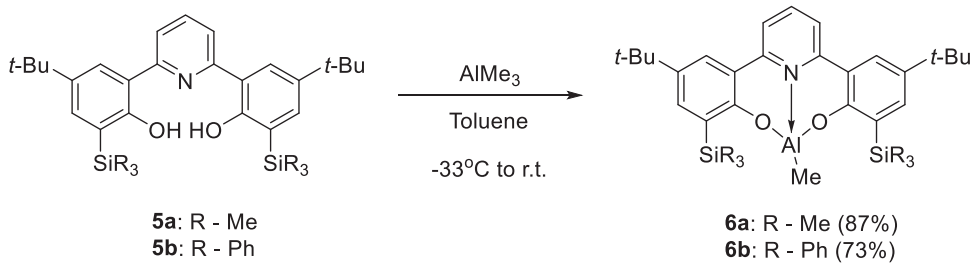

5a: R - Me
5b: R - Ph

6a: R - Me (87%)
6b: R - Ph (73%)

Scheme 2. Synthesis of aluminum complexes **6a** and **6b**.

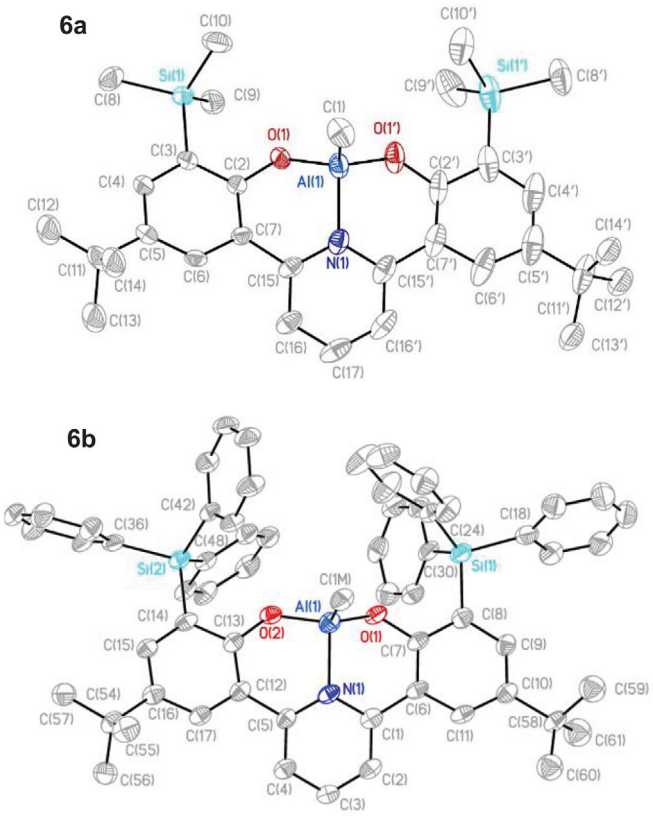

Figure 2. Molecular structure of **6a**. All hydrogens atoms are hidden. Selected bonds distances(Å) and angles: Al1-O1 1.752(3), Al1-O1′ 1.740(3), Al1-C1 1.921(5), Al1-N1 1.914(4), O1-Al1-O1′ 111.0(1), O1-Al1-N1 96.2(1), O1′-Al1-N1 97.0(1), O1-Al1-C1 117.2(2), O1′-Al1-C1 116.6(2), N1-Al1-C1 115.3(2). Molecular structure of **6b**. All hydrogens atoms are hidden. Selected bond lengths (Å) and angles: Al1-O1 1.755(3), Al1-O2 1.754(3), Al1-C1M 1.933(4), Al1-N1 1.950(3), O1-Al1-O2 112.5(2), O1-Al1-C1M 118.0(2), O2-Al1-C1M 118.6(2), O1-Al1-N1 95.4(1), O2-Al1-N1 95.3(1), C1M-Al1-N1 111.8(2).

2.3. Ring Opening Polymerization of ε-Caprolactone, *rac*-Lactide, and L-lactide

As mentioned above, a comparative study of polymerization under the action of **C**,[10c] **6a** (this work), and **6b** (this work) in the presence of an external nucleophile was of great interest. According to the generally accepted mechanism of polymerization by the "coordination–insertion" mechanism, which is supported by calculation data,[6,7b,7d,8] at the first stage, (after the conversion of the methyl complex into a benzyloxy derivative) there is an attack of the oxygen atom of the carbonyl group on the aluminum atom with the formation of a transition state (TS),[8f,g,13] in which the aluminum atom is pentacoordinated. Moreover, the attack can occur both from the side opposite to the nitrogen atom (axial attack, in the resulting TS, which is a trigonal bipyramid, the oxygen atom of the carbonyl group is in the axial position, as well as the nitrogen atom), and as an attack in the R—Al—N plane, when the oxygen atom is attached to the aluminum atom between the Al—R and Al—N bonds, ending up in the equatorial position of the TBP (equatorial attack, the axial positions are occupied by the R substituent and the nitrogen atom) (Figure 3a). Figure 3a also shows the structures of compounds **C**, **6a,** and **6b** with the display of van der Waals radii of the atoms. It can be confidently assumed that the replacement of the methyl group by the OR group, which is required according to the "coordination–insertion" mechanism, should not lead to a significant rearrangement of the initiator structure. When going from **C** (*t*-Bu substituents) to **6a** (Me_3Si substituents), no significant changes in the structure occur, it should be noted only the lengthening of the Si—C bond in the Me_3Si groups compared to the C—C bond in the *t*-Bu groups. There is also a slight decrease in the catalytic pocket by 1.9 (Figure 3b), which is confirmed by an increase in the reduced density gradient (Figure 3c) and the intensity of peaks (Figure 3d) of the van der Waal interactions (green) between methyl groups of *t*-Bu and $SiMe_3$ substituents and methyl group on Al atom and oxygen atoms of ligands.

A significant change in the structure of the initiator occurs in the transition from **6a** to **6b**, the phenyl rings prevent both axial attack and equatorial attack, and despite the apparent possibility of equatorial attack, it requires further displacement of the R group to the axial position, which is hindered by the phenyl groups. The steric proximity of the phenyl rings and the R substituent (in **6b** – a methyl group) is confirmed by the shift of the methyl group signal in the ^{1}H NMR spectrum to a strong field (–1.71 ppm). The catalytic pocket decreases significantly by 15.6, the red zones indicate the more-hindered catalytic reaction center in **6b** (Figure 3b). Also, significant increase in the reduced density gradient (Figure 3c) and the intensity of peaks (Figure 3d) of the van der Waal interactions occurs due to steric clashes of the phenyl rings among themselves and with methyl group on Al atom and oxygen atoms of ligands.

Percent buried volume (%V_{Bur}) highlights a difference in steric bulkiness between ligands in three considered initiators, with the tBu-substituted ligand in **C** less bulky and $SiPh_3$-substitited ligand in **6b** clearly most bulky. Comparison of the steric maps of initiators **C**, **6a,** and **6b** indicated that the steric hindering of the reaction center in **6a** and especially in **6b** should lead to some

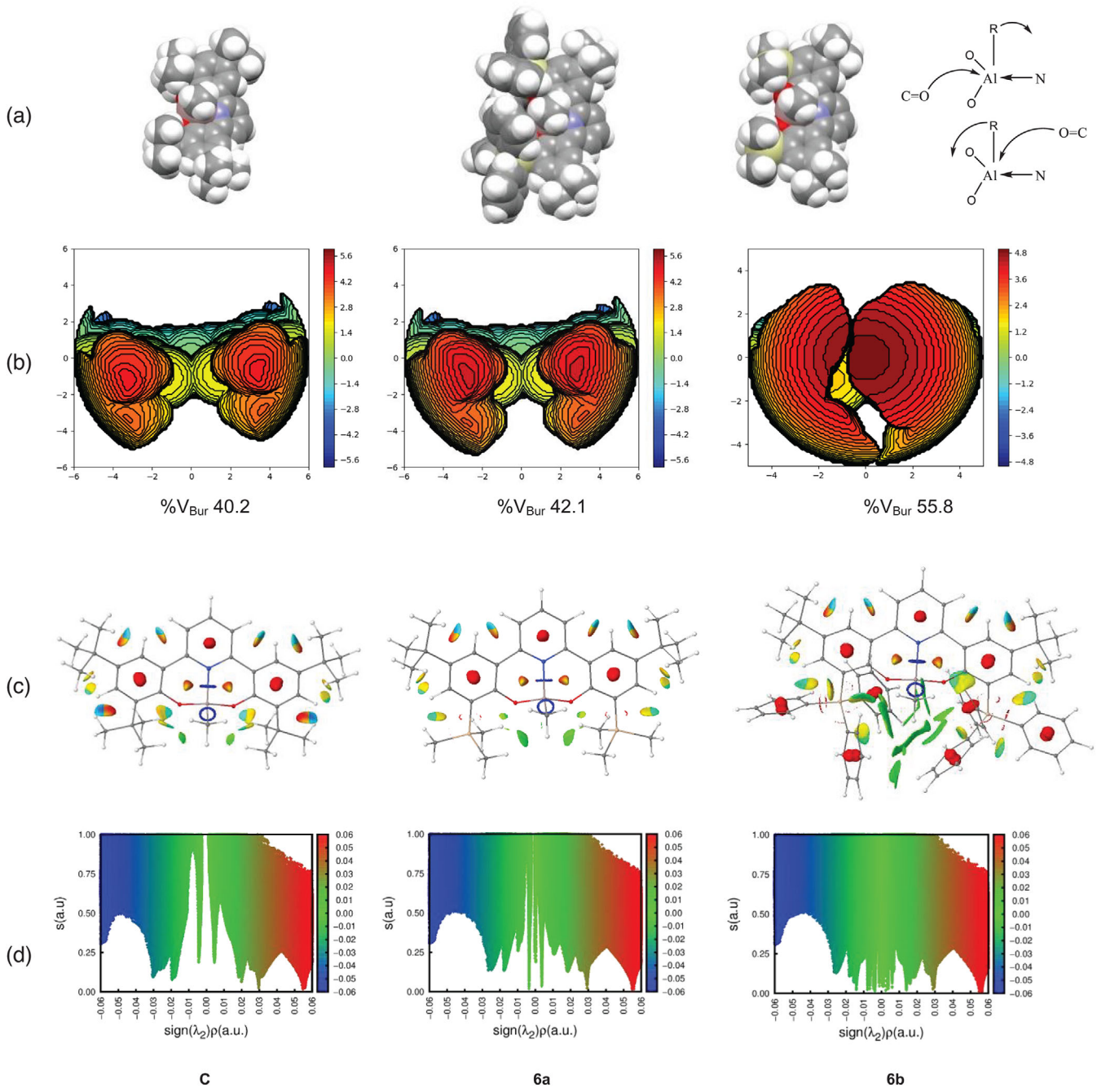

Figure 3. (a) Comparison of the structures of **C** (X-ray diffraction data), **6a,** (X-ray diffraction data) and **6b** (calculated data), and the direction of possible nucleophile attack during polymerization. (b) Steric maps and percent buried volumes (%V_{Bur}, sphere radius 6 Å) of initiators **C**, **6a**, and **6b**. The steric maps are viewed down the *z*-axis and *z*-axis is selected along the Al—N bond. (c) s(r) isosurfaces (cut-off 0.3 a.u.) and (d) corresponding 2D plots colored by sign(λ2)ρ(r) for initiators **C**, **6a**, and **6b**.

increase in the difficulties of attack from both axial and equatorial side, that is, to some slowing down of polymerization in the case of **6a** and especially of **6b** compared to **C** (this is confirmed by the results of quantum-chemical calculations, see below).

Homopolymerization studies of *rac*-LA (Table 1, *entries* 1–4) and L-LA (Table 1, entries 5–9) with complexes **6a** and **6b** were performed with BnOH as co-initiator. Compound **6a** demonstrated higher activity in all entries except high temperature L-LA polymerization (*entries* 8 and 9). Comparison of the activities of**C**[10c] and **6a** shows that they are close. The lower results compared to the theoretical molecular weights in both cases (*entries* 8 and 9) can presumably be explained by the thermal destruction of the polymers under polymerization conditions. Low activity of **6b** in toluene solutions (*entries* 4 and 7) may be due to itslow solubility. The molecular weight distributions as determined by GPC were significantly narrow ($Đ$ = 1.10—1.39). These data illustrate the good degree ofcontrol over the molecular weights provided by these in situ generated alkoxy-aluminum

Table 1. Ring opening polymerization of lactides promoted by complexes **6a** and **6b**.

Entry	Initiator	Conditions	Conversion[d]	Time, h	$M_{n,GPC}$[e]	$M_{n,theor}$[f]	$Đ$[e]	P_m[g]
rac-LA								
1[a]	**6a**	In bulk, 130 °C	95%	0.5h	–[h]	–	–	–
			98%	1h	11,667	14,220	1.39	0.51
2[a]	**6b**		78%	0.5h	–	–	–	–
			98%	1h	9431	14,220	1.20	0.52
3[a]	**6a**	Toluene, 80 °C, [LA] = 1M	8	1h	–	–	–	–
			19	3h	–	–	–	–
			43	6h	–	–	–	–
			90	24h	11,941	13,068	1.32	0.46
4[a]	**6b**		8%	1h	–	–	–	–
			13%	3h	–	–	–	–
			20%	6h	–	–	–	–
			41%	24h	–	–	–	–
			48%	72h	–	–	–	–
			81%	96h	2267	11,770	1.06	0.49
L-LA								
5[a]	**6a**	In bulk, 100 °C	36%	0.5h	–	–	–	–
			57%	1h	–	–	–	–
			96%	3h	–	–	–	–
			100%	6h	13,288	14,500	1.17	–
6[a]	**6b**		11%	1h	–	–	–	–
			76%	3h	–	–	–	–
			100%	6h	15,955	14,500	1.17	–
7[b]	**6b**	Toluene, 80 °C, [LA] = 1M	11%	1h	–	–	–	–
			20%	3h	–	–	–	–
			46%	6h	–	–	–	–
			85%	24h	–	–	–	–
			100%	48h	5841	7300	1.10	–
8[c]	**6a**	In bulk, 140 °C	1%	3h	–	–	–	–
			3%	6h	–	–	–	–
			9%	24h	–	–	–	–
			24%	48h	–	–	–	–
			53%	120h	–	–	–	–
			71%	144h	6484	204,500	1.26	–
9[c]	**6b**		1%	3h	–	–	–	–
			9%	6h	–	–	–	–
			19%	24h	–	–	–	–
			48%	48h	–	–	–	–
			81%	82h	–	–	–	–
			88%	120h	5422	253,500	1.35	–

[a] [LA]:[Initiator]:[BnOH] = 100:1:1;
[b] [LA]:[Initiator]:[BnOH] = 50:1:1;
[c] [LA]:[Initiator]:[BnOH] = 2000:1:1;
[d] determined by ^{1}H NMR in $CDCl_3$;
[e] determined by GPC in THF using polystyrene standards for calibration and correction factor 0.58;[15]
[f] $M_{n,theor} = 144 \times [LA] \times$ conversion/100 + 108;
[g] determined by ^{1}H NMR homodecoupling experiments in methine area;[4d,16]
[h] $M_{n,GPC}$,$M_{n,theor}$, $Đ$, P_m were determined only for isolated polymers.

Table 2. Ring opening polymerization of ε-caprolactone promoted by complexes **6a** and **6b**.

Entry	Initiator	Conditions	Conversion[c]	Time, h	$M_{n,GPC}$[d]	$M_{n,NMR}$[c]	$M_{n,theor}$[e]	$Đ$[d]
10[a]	**6a**	In bulk, 100 °C	99%	0.25	16,264	6378	11,394	1.52
11[a]	**6b**		99%	0.25	10,192	10,026	11,394	1.55
12[a]	**6a**	Toluene, 25 °C, [CL] = 1M	45%	1h	–[f]	–	–	–
			98%	3h	16,423	6720	11,280	1.29
13[a]	**6b**		3%	0.5h	–	–	–	–
			6%	1h	–	–	–	–
			34%	3h	–	–	–	–
			35%	24h	–	–	–	–
14[a]	**6b**	Toluene, 80 °C, [CL] = 1M	99%	0.5h	10,192	9000	11,394	1.47
15[b]	**6a**	In bulk, 140 °C	0%	1h	–	–	–	–
			4%	3h	–	–	–	–
			10%	6h	–	–	–	–
			16%	24h	–	–	–	–
			65%	48h	–	–	–	–
			99%	96h	21,659	29,450	225,828	1.50
16[b]	**6b**		2%	0.5h	–	–	–	–
			4%	1h	–	–	–	–
			27%	3h	–	–	–	–
			39%	6h	–	–	–	–
			90%	24h	–	–	–	–
			96%	48h	35,726	46,673	218,988	1.76

[a] [ε-CL]:[Initiator]:[BnOH] = 100:1:1;
[b] [ε-CL]:[Initiator]:[BnOH] = 2000:1:1;
[c] Determined by ^{1}H NMR in $CDCl_3$, $M_{n,NMR}$ = I(CH_2Ph)PCL × M_w(CL) + M_w(BnOH);
[d] Determined by GPC in THF using polystyrene standards for calibration and correction factor 0.56;[15c]
[e] $M_{n,theor}$ = 114×[CL]×conversion/100 + 108;
[f] $M_{n,GPC}$,$M_{n,theor}$, $Đ$, P_m were determined only for isolated polymers;

complexes. The structure of complexes **6a** and **6b** does not show the ability to influence the tacticity of the resulting polymer; the obtained PLA samples demonstrate P_m values of about 0.46–0.52. The degree of isotacticity of PLA in the polymerization of rac-LA (P_m value) was determined based on the methine region of homonuclear ^{1}H{^{1}H} NMR spectroscopy based on the Bernoulli distribution (seeSupporting information, FiguresS21–S24).

In order to study the structure of the resulting PLA, it was decided to provide an experiment in the ratio [LA]:[Initiator]:[BnOH] = 50:1:1 to obtain low molecular weight polymer. A MALDI-TOF experiment was performed on the isolated product of *entry* 7 (Supporting Information, Figure S18). The mass spectrum is characterized by a set of peaks separated by corresponding repeating unit molar masses of LA. The peak difference of 144 Da indicates the absence of transesterification during the polymerization of L-LA.[14] Analysis MALDI-TOF of PLA showed a peak at $[M+Na]^+$ (3587.987 Da, Figure S18) resulting from a polymer with degree of polymerization (DP = 24) having BnO- and -OH terminal groups.

The ability of **6a** and **6b** to promote the ROP of CL also was examined. Homopolymerization studies of ε-CL with complexes **6a** and **6b** were performed in the presence of BnOH as co-initiator in bulky conditions at 100 °C (Table 2, *entries* 10, 11). They both performed very well, giving a full conversion in 15 min. Both complexes give quite similar molecular weights and $Đ$. Similar results were obtained for complex **C**, although its greater activity compared to **6a** should be noted.[10c] To study the kinetics of the polymerization process, it was decided to investigate polymerization at room temperature in toluene solution. In the case of **6b**, it was not possible to isolate the polymer (*entry* 13). The low activity of **6b** may also be related to the low solubility of **6b** in toluene at room temperature. But at 80 °C the solubility of **6b** increases, and this initiator transforms 99% of monomer to polymer during 30 min (*entry* 14).

Polymerizations of L-LA (*entries* 8–9) and CL (*entries* 15–16) with low initiator loads ([monomer]:[initiator] = 2000:1) at high temperature (**6b** is stable under 300 °C according TG data (see Figure S18, Supporting Information) also have been investigated. Initiators **6a** and **6b** showed low activity in the polymerization of LA under these conditions. In contrast to the inefficiency found for **6a** and **6b** in the synthesis of PLA with small initiator loadings, both initiators showed good results in the synthesis of PCL. It is also worth noting that we do not observe a significant increase in the molecular weight of PLA and PCL with an increase in the molar ratio of monomer to initiator, which is associated with transesterification as a result of long-term

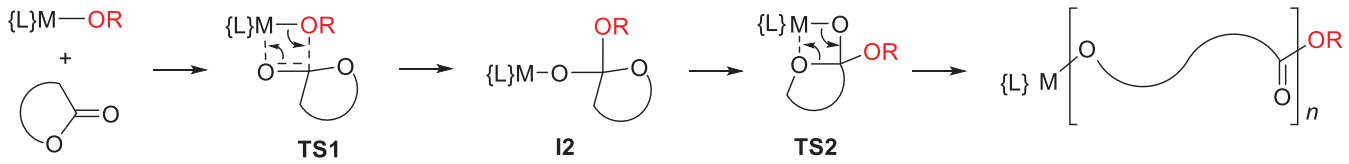

Scheme 3. The simplified coordination–insertion mechanism of ROP.

thermal exposure. As for a possible explanation for the higher activity of **6b** under these harsh conditions, it should be noted that the activation energy values for **6a** and **6b** in the first stage of the process (see below) do not differ very significantly and, apparently, other factors begin to have an influence.

Our attempts to obtain co-polymers of LA and CL at 100 °C were unsuccessful ([CL]:[LA]:[Initiator]:[BnOH] = 100:100:1:1).

2.4. DFT Calculations

The mechanism of ROP mediated by metal alkoxide complexes is well investigated and described by the coordination-insertion process (Scheme 3),[8,17] in which two stages are involved: the addition of the monomer to the metal catalytic center with subsequent attack by alkoxy group of carbonyl carbon atom (**TS1**) and the lactone cycle opening with forming new metal alkoxide at the chain-end (**TS2**). Depending on the coordination capabilities of the metal, a number of intermediates can be formed, such as complexes of the initiator or product with the coordination of the carbonyl oxygen atom at the metal atom and intermediates with four-membered cycles —Al—O—C—O—.[8f,g] We used the DFT calculation based on the coordination-insertion mechanism to rationalize the ε-CL polymerization catalyzed by complexes **C**, **6a**, and **6b**.

Gibbs free energy surfaces of the initiation step in ROP of CL are presented in Figure 4. Methanol was chosen as co-initiator to simplify calculations. Prior to the reaction, a complex is formed between the reactants. It can be van-der-Waals complex (**RC_vdW**) or complex with coordination of monomer by carbonyl oxygen at metal atom (**RCax**), depending on their relative stability. As mentioned above, the addition of monomer can proceed via equatorial or axial position of initiator (see. Figure 3a), and only formation of complexes with axial addition of monomer is profitable (**RCax**). Then transfer of the alkoxy group from the metal atom to the carbonyl carbon atom of monomer is carried out through four-membered cyclic transition states (**TS1ax**, **TS1eq**). This stage is rate limiting and Gibbs free energy activation barriers are 10.1, 11.1, 13.9 kcal mol^{-1} for equatorial addition of monomer and 12.8, 13.3, 18.0 kcal mol^{-1} for axial addition of monomer for reactions with initiators **C**, **6a**, **6b** respectively. It should be noted that the equatorial path is more profitable for all initiators due to lower steric hindrance for equatorial attack of monomer.

The changes in the volume of the catalytic pocket, as well as non-covalent interactions in it, were analyzed for **TS1eq** and compared with the free initiators **C**, **6a**, and **6b**. Insertion of monomer to the complex to form the **TS1eq**, as expected, leads to an increase in the catalytic pocket size and a decrease in %V_{Bur} in comparison with free initiators by 0.9, 1.3, and 4.5 for **C**, **6a**, **6b**, respectively (Figure S21a). This change is the greatest in **6b**. The intensity of van-der-Waals interactions also increases in all transition states in comparison with free initiators (Figures S21b and S21c). The most significant bulkiness of ligands occurs in **6b** resulting in more distorted structure around metal atom and increase in Gibbs free activation energy of the **TS1eq**.

The polymerization reaction takes place most often in bulk, but we also carried out the reaction in toluene. The solvent effect can play a critical role in CL polymerization processes, although, for toluene the Gibbs energy profiles show a similar trend as in the gas-phase.[7a] In order to determine the effect of the solvent on the activation barriers of the reaction, we performed a calculation in the solvent medium (Figure 4). Toluene does not capable to form strong specific intermolecular interactions, so the solvation model based on density (SMD)[18] is sufficient to simulate the medium. The calculations showed that for the reactions under consideration, the patterns found in gas-phase remain unchanged. We note only a decrease in the difference in activation barriers of the reactions with three initiators and less stability of most intermediates **I1**, **I2**, **I3** for the reaction in toluene.

A number of intermediates (**I1**, **I2**, **I3**) are formed as a result of first stage. Transitions between **I1**, **I2**, **I3** occur by the mechanism of dissociation of coordination bonds and conformational rotation around single bonds. The potential surface at this location is very flat and the transition barriers between such structures are below 1 kcal/mol. The lactone cycle cleavage occurs through **TS2** with Gibbs free energy barriers of 12.0, 11.9, 12.6 kcal mol^{-1} for equatorial position of carbonyl O atom and 0.6, 1.8, 1.9 kcal mol^{-1} for axial position of carbonyl O atom for reactions with initiators **C**, **6a**, **6b** respectively. Both paths proceed through **I2** and the stage 2 can father proceed through any **TS2ax** or **TS2eq**.

Gibbs free energy surfaces of ROP of CL mediated by complexes **C**, **6a**, and **6b** indicated that the steric volume of substituents nearly reaction center have a great influence on the reaction rate. The bulkiness of substituents increases activation barriers and slows the reaction, which is also consistent with experimental data. Complex **6a** shows a higher increase in the conversion of polymerization of LA and CL under similar conditions than complex **6b** (see Supporting Information, Figure S25).

3. Conclusions

In the course of the work, two Al-containing initiators of the ROP of L-LA and CL based on 2,6-bis(2-hydroxy-3,5-di(*t*-butyl)phenyl)pyridine were obtained and fully characterized.

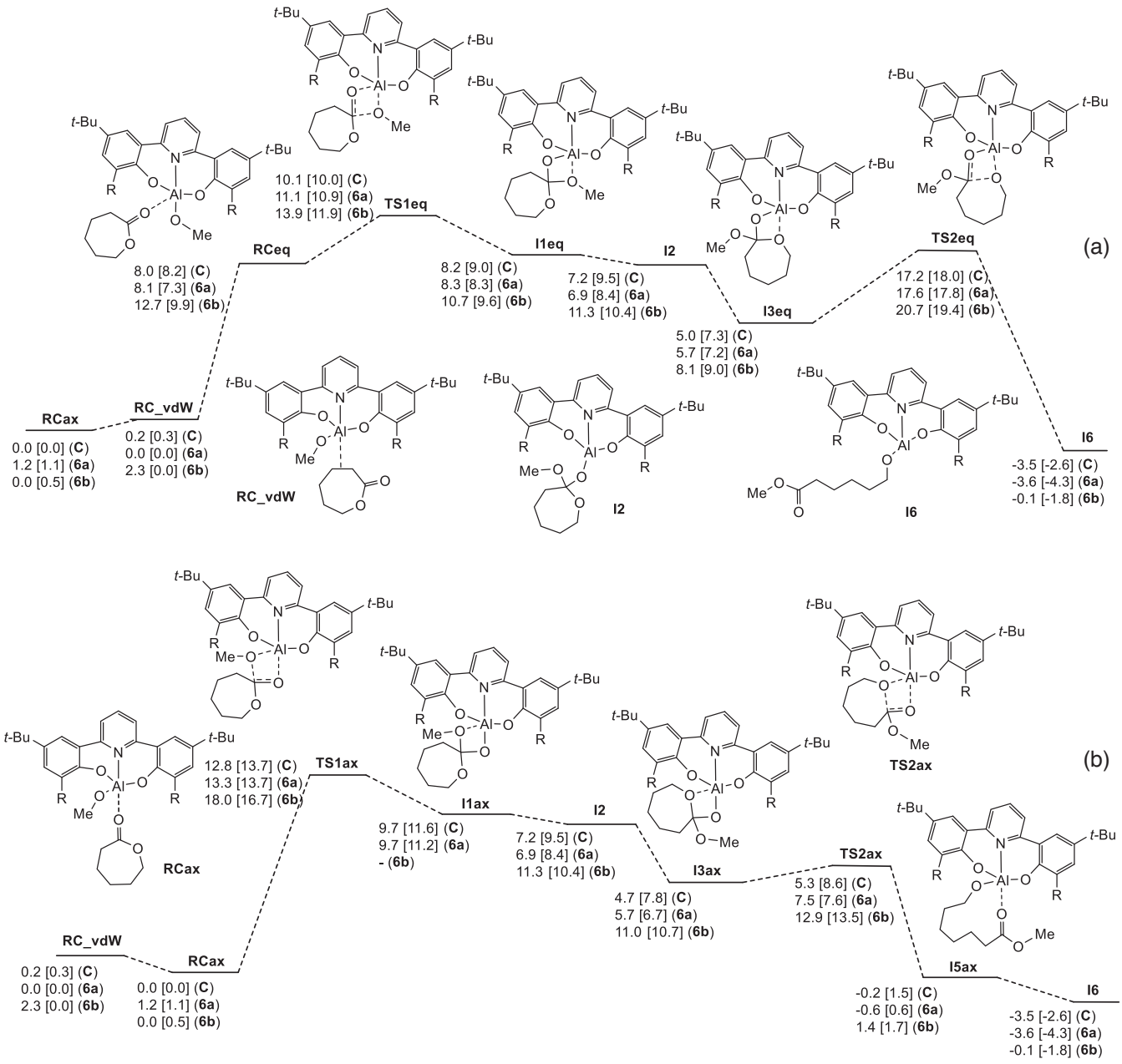

Figure 4. Gibbs free energy profiles of initiation stages of CL polymerization proceeding with (a) equatorial and (b) axial monomer addition to initiator. The values in square brackets correspond to the reaction in toluene.

We demonstrated that these complexes containing substituents with different steric volume can be effective initiators for the production of PCL and PLA homopolymers with relatively narrow dispersion and controlled molecular weights of polymers under various conditions. It should be noted that a greater number of substituents near the metal center slows down the reaction.

We have made a detailed DFT calculation of the initiation stage of mechanism of ROP of CL catalyzed by initiators with different bulkiness of substituents at the reaction center and found the significant influence of steric effect on the polymerization rate. The activation Gibbs free energy increases with NCI increase and steric volume of catalytic pocket decrease in the order of substituents *t*-Bu<$SiMe_3$<$SiPh_3$ in accordance with the increase in bulk. The calculated activation barriers correspond to the reaction rate dependencies found experimentally.

4. Experimental Section

4.1. Experimental Details

All reactions with air- and/or water-sensitive compounds were performed under a dry, oxygen-free, argon atmosphere using standard Schlenk techniques. Solvents were dried by standard methods and distilled prior to use: toluene and *n*-hexane were refluxed over Na and distilled; THF, and Et_2O were refluxed over Na/benzophenone and distilled; BnOH was distilled under vacuum and kept over acti-

vated 4 Å molecular sieves. $AlMe_3$ (2.0 M solution in toluene, Sigma–Aldrich), *n*-BuLi (Sigma–Aldrich), $SiMe_3Cl$ (≥99% Sigma–Aldrich), Ph_3SiCl (99%, Sigma–Aldrich), $ZnCl_2$, MeOH (99%, Sigma–Aldrich), EtOAc (99%, Sigma–Aldrich), Na_2SO_4 (99%, Sigma–Aldrich), Na_2SO_3 (99%, Sigma–Aldrich), CH_2Cl_2 (99%, Sigma–Aldrich) were used as purchased. L-LA (98%, Sigma–Aldrich) and *rac*-LA (98%, Sigma–Aldrich) were recrystallized from toluene and sublimed *in vacuo*, CL (97%, Sigma–Aldrich) was distilled over CaH_2. $CDCl_3$ (dried with CaH_2 and kept over activated 4 Å molecular sieves.) was obtained from Deutero GmbH (Kastellaun, Germany).

^1H (400.13 MHz) and ^{13}C (100.61 MHz) NMR spectra were recorded on a Bruker Avance 400 (Bruker Corporation, Billerica, MS, USA) or Agilent 400-MR (Agilent Technologies, Santa Clara, CA, USA) spectrometers at room temperature ^1H and ^{13}C chemical shifts are reported in ppm relative to Me_4Si as an internal standard. Elemental analysis was performed using EuroEA-3000 instrument (EuroVector, Pavia, Italy). High-resolution mass spectra (HRMS) were recorded on a Bruker micrOTOF II instrument using electrospray ionization (ESI). A sample of about 5 mg of an aluminum complex based on a pyridine-containing ligand was placed in an aluminum oxide ceramic crucible and then in the furnace of a simultaneous thermal analysis device STA 449 C Jupiter (NETZSCH, Germany). Before measurements, the furnace was evacuated three times and purged with argon for an hour. After this, the following gas flows were established: active argon flow 80 ml/min, shielding gas flow (to protect the weighing unit) argon 40 ml/min. Then it was heated at a speed of 1 degree/min to 40C and kept in standby mode for 20 min until the scale readings were established. Then it was heated at a rate of 10 degrees/min to 1000C, simultaneously recording the thermogravimetry (TG), diferential thermal analysis (DTG), and diferential scanning calorimetry (DSC) signals. Baseline correction for empty cup measurements was used. The apparent molecular weight characteristics of the polymers were determined via GPC on a 1260 Infinity II GPC/SEC Multidetector System chromatograph (Agilent, Santa Clara, CA, USA) equipped with two PLgel 5 μm MIXED B columns ($M = 5 \times 10^2$–1×10^7), at 40 °C in THF at a flow rate of 1 mL min^{-1}. Average molecular weights were calculated using narrowly dispersed standards of polystyrene. Matrix-assisted laser desorption/ionization mass spectrometry (MALDI MS): MALDI experiments were performed using Bruker autoflex speed time-of-flight (TOF) mass spectrometer (Germany) equipped with a solid-state UV-laser ($\lambda = 355$ nm) and operated in positive ion linear mode. Matrix solution (HCCA, 30 mg/ml in THF) was pre-mixed with the sample solutions (10 mg/mL in THF) in a ratio of 5/1(v/v), spotted on a steel targets (MTP 384 ground steel; Bruker Daltonics Inc., Germany) and air-dried. At least 200 single spectra were recorded at different positions within the spots using laser power ranged from 70% to 90%.

Quantum chemical calculations were carried out at the density functional theory (DFT) level of theory using the nonempirically generalized gradient approximation and the PBE functional[19] in the TZ2P basis implemented in PRIRODA program.[20] The geometry optimization to find the energy minimum was performed for all stable complexes and intermediates (I); the saddle point search method was performed for the transition states (TS). The characters of the stationary points found (minima or saddle point on the PES) were determined by calculating the eigenvalues of the matrix of the second energy derivatives with respect to the nuclear coordinates. Correspondence between a particular TS and a transformation under study was verified by calculating the intrinsic reaction coordinate (IRC). For all structures, the conformational analysis was performed to find structures with minimal energy. The reported Gibbs free energy values (kcal·mol^{-1}) correspond to conformers with minimal energy, are sums of the electronic energy, heat corrections (298 K), dispersion corrections (PBE-D4),[21] and solvation energy for reaction in toluene. The Gibbs free activation energy values are calculated relative to the most stable structures (ground state), preceding the TS on each stage, which are the most stable complexes of reagents for **TS1** or the most stable intermediates for **TS2**. The non-covalent interactions (NCI) were analyzed using the NCIweb server (https://nciweb.dsi.upmc.fr/)[22] and with using promolecular density approximation.[23] Solvent effects in toluene using the SMD method[18] were calculated in the ORCA Ver. 6[24] program package and PBE[19] functional in def2-TZVP[25] basis set as single point calculations of PBE/TZ2P optimized geometries.

4.1.1. Synthesis of Ligands

Synthesis of 2,6-dibromo-4-(t-butyl)phenol (1): To a stirred solution of 4-(*t*-butyl)phenol (10.00 g, 0.067 mol) in CH_2Cl_2 (200 ml) in two-necked flask (250 ml), bromine (7.4 ml, 0.143 mol) was added drop-wise at room temperature. The reaction mixture was stirred overnight. Excess of bromine was neutralized by aqueous solution of Na_2SO_3. Organic layer was washed with brine (3 × 50 mL) and dried over Na_2SO_4. The resulting mixture was filtrated and concentrated under reduced pressure to provide colorless crystals of **1** (m = 20.39 g, yield 99%, MP 71 °C). MP, ^1H, and ^{13}C NMR data are in the accordance with literature.[26]

Synthesis of 1,3-dibromo-5-(t-butyl)-2-(methoxymethoxy)-benzene (2): To a stirred solution of **1** (19.51 g, 0.063 mol) in anhydrous THF (200 mL), NaH (3.34 g, 0.139 mol) was carefully added at 0 °C. After stirring for 1 h at room temperature, MOMCl (obtained using the described procedure[27]) (5.68 g, 0.070 mol) was added dropwise, the resulting mixture was stirred by 2 days at room temperature. Then water (15 mL) was carefully added at room temperature THF was removed by evaporation, the mixture was dissolved in EtOAc (100 mL). Combined organic layer was washed with brine (3 × 50 mL) and dried over Na_2SO_4. The resulting mixture was filtrated and concentrated under reduced pressure to provide light-yellow oil **2** (m = 19.85 g, yield 89%). ^1H and ^{13}C NMR data are in the accordance with literature.[28]

Synthesis of (3-bromo-5-(t-butyl)-2-(methoxymethoxy)phenyl)-trimethylsilane (3a): To a stirred solution of **2** (7.61 g, 0.022 mol) in anhydrous Et_2O (90 mL), *n*-BuLi (9.70 ml of a 2.5 M solution in hexane, 0.024 mol) was slowly added at −78 °C. After stirring for 30 min at -−78 °C, $SiMe_3Cl$ (2.58 g, 0.024 mol) was added drop-wise. The mixture was slowly heated to room temperature, and stirred overnight. Then water was added to dissolve all precipitate. Water fraction was extracted by EtOAc (3 × 25 mL). The combined organic layer was washed with brine (3 × 40 mL), dried over Na_2SO_4 and finally evaporated to afford as a yellow oil (m = 7.17 g, 96%).

^1H NMR ($CDCl_3$, δ, ppm): 0.32 (s., 9H, $Si(CH_3)_3$), 1.29 (s., 9H, $C(CH_3)_3$), 3.64 (s., 3H, OCH_3), 5.11 (s., 2H, OCH_2O), 7.35 (d., 1H, Ar, $J = 2.38$ Hz), 7.53–7.54 (d., 1H, Ar, $J = 2.38$ Hz). ^{13}C NMR ($CDCl_3$, δ, ppm): -0.19 ($Si(CH_3)_3$), 31.31 ($C(CH_3)_3$), 34.41 ($C(CH_3)_3$), 57.91 (OCH_3), 99.49 (OCH_2O), 116.33, 131.40, 132.05, 134.93, 148.28, 155.74 (Ar). Anal. calc. for $C_{15}H_{25}BrO_2Si$: C, 52.17; H, 7.30. Found C, 52.30; H, 7.34.

(3-bromo-5-(t-butyl)-2-(methoxymethoxy)phenyl)triphenylsilane (3b): This compound was prepared following the same procedure as that described above for **3a** starting from **2** (5.00 g, 0.014 mol), *n*-BuLi (5.95 mL of a 2.5 M solution in hexane, 0.015 mol) and Ph_3SiCl (4.19 g, 0.014 mol). The crude product was purified by column chromatography on silica gel (toluene: petroleum ether = 1:1, $R_f = 0.36$)

to provide compound **3b** as white solid (m = 4.09 g, 54%, MP 160 °C).

^{1}H NMR ($CDCl_3$, δ, ppm): 1.13 (s., 9H, C(CH_3)$_3$), 3.06 (s., 3H, OCH_3), 4.31 (s., 2H, OCH_2O), 7.20–7.21 (d., 1H, Ar, *J* = 2.74 Hz), 7.35–7.42 (m., 10H, Ar), 7.58–7.60 (m., 5H, Ar), 7.63 (d., 1H, Ar, *J* = 2.35 Hz). ^{13}C NMR ($CDCl_3$, δ, ppm): 31.10 (C(**C**H_3)$_3$), 34.36 (**C**(CH$_3$)$_3$), 57.41 (O**C**H$_3$), 98.35 (O**C**H$_2$O), 116.63, 127.53, 127.76, 129.58, 133.35, 134.30, 135.29, 136.48, 148.11, 155.77 (Ar). Anal. calc. for $C_{30}H_{31}BrO_2Si$: C, 67.79; H, 5.88. Found C, 67.90; H, 5.95.

2,6-bis(5-(t-butyl)-2-(methoxymethoxy)-3-(trimethylsilyl)phenyl)-pyridine (4a): To a stirred solution of compound **3a** (3.75 g, 0.011 mol) in anhydrous THF (35 ml), *n*-BuLi (4.80 mL of a 2.5 M solution in hexane, 0.012 mol) was slowly added at -78 °C. After stirring for 1 h at −78 °C, a solution of anhydrous $ZnCl_2$ (1.97 g, 0.014 mol) in anhydrous THF (25 mL) was added dropwise at -78 °C, then the mixture was stirred for 30 min and carefully heated to room temperature. A solution of $Pd(PPh_3)_4$ (0.13 g, 0.109 mmol) in anhydrous THF (6 mL) and a solution of 2,6-dibromopyridine (0.85 g, 0.004 mol) in anhydrous THF (6 mL) were added at room temperature. The mixture was refluxed for 16 h. After cooling to room temperature, water was added. The water fraction was extracted by EtOAc (3 × 50 mL), the combined organic layer was washed with brine (3 × 50 mL), then dried over Na_2SO_4. After filtration and concentration under reduced pressure, the crude product was purified by column chromatography on silica gel (toluene: petroleum ether = 4:1, R_f = 0.35) to give **5a** as light-yellow solid (m = 0.97 g, 44%, MP 160 °C–165 °C).

^{1}H NMR ($CDCl_3$, δ, ppm): 0.37 (s., 18H, Si(CH_3)$_3$), 1.36 (s., 18H, C(CH_3)$_3$), 3.28 (s., 6H, OCH_3), 4.67 (s., 4H, OCH_2O),7.50 (d., 2H, Ar, *J* = 2.74 Hz), 7.72–7.74 (m., 3H, Ar), 7.83–7.84 (d., 2H, Ar, *J* = 2.74 Hz). ^{13}C NMR ($CDCl_3$, δ, ppm): −0.09 (Si(CH_3)$_3$), 31.43 (C(CH_3)$_3$), 34.45 (C(CH$_3$)$_3$), 57.41 (OCH_3), 99.79 (OCH_2O), 122.87, 130.11, 132.42, 132.89, 132.95, 135.86, 146.36, 157.19, 157.41 (Ar). Anal. calc. for $C_{35}H_{53}NO_4Si_2$: C, 69.14; H, 8.79; N, 2.30. Found: C, 69.50; H, 8.69; N, 2.35.

2,6-bis(5-(t-butyl)-2-(methoxymethoxy)-3-(triphenylsilyl)phenyl)-pyridine (4b): This product was prepared as described above for **4a** starting with **3b** (4.05 g, 0.0076 mol), *n*-BuLi (3.35 mL of a 2.5 M solution in hexane, 0.0084 mol), $ZnCl_2$ (1.38 g, 0.0101 mol), $Pd(PPh_3)_4$ (0.088 g, 0.076 mmol), 2,6-dibromopyridine (0.60 g, 0.0025 mol). The resulting crude was purified by column chromatography on silica gel (ethyl acetate: petroleum ether = 1:15, R_f = 0.25) to give **4b** as a white powder (m = 1.85 g, 75%, MP 155 °C–157 °C).

^{1}H NMR ($CDCl_3$, δ, ppm): 1.19 (s., 18H, C(CH_3)$_3$), 2.62 (s., 6H, OCH_3), 3.89 (s., 4H, OCH_2O), 7.30–7.31 (d., 2H, Ar, *J* = 2.63 Hz), 7.33–7.42 (m., 18H, Ar), 7.62–7.64 (dd., 12H, Ar, *J* = 1.50 Hz, *J* = 6.48 Hz), 7.72–7.74 (t., 3H, Ar, *J* = 3.36 Hz), 7.87 (d., 2H, Ar, *J* = 2.63 Hz). ^{13}C NMR ($CDCl_3$, δ, ppm): 31.21 (C(CH_3)$_3$), 34.37 (C(CH$_3$)$_3$), 56.76 (OCH_3) 98.75 (OCH_2O) 123.19, 127.63, 127.89, 129.36, 131.27, 133.05, 134.94, 135.72, 136.52, 136.68, 146.38, 157.03, 157.20 (Ar). Anal. calc. for $C_{65}H_{65}NO_4Si_2$: C, 79.63; H, 6.68; N, 1.43. Found C, 79.80; H, 6.65; N, 1.45.

6,6′-(pyridine-2,6-diyl)bis(4-(t-butyl)-2-(trimethylsilyl)phenol) (5a): To a stirred solution of compound **4a** (0.50 g, 0.82 mmol) in THF (3 mL), an HCl_{conc} (0.86 mL, 9.9 mmol) was added at room temperature. The resulting mixture was stirred for 1 h. After that, the mixture was quenched with water (5 mL) and extracted by Et_2O (3 × 10 mL). The combined organic layer was washed with $NaHCO_3$ solution, dried over Na_2SO_4 and concentrated under reduced pressure to give compound **5a** as a light-green powder (m = 0.36 g, 84%).

^{1}H NMR ($CDCl_3$, δ, ppm): 0.32 (s., 18H, Si(CH_3)$_3$), 1.36 (s., 18H, C(CH_3)$_3$), 7.48–7.49 (d., 2H, Ar, *J* = 2.45 Hz), 7.63–7.66 (m., 4H, Ar), 7.97–8.01 (t., 1H, Ar, *J* = 7.95 Hz), 10.28 (s., 1H, O**H**). ^{13}C NMR ($CDCl_3$, δ, ppm): -1.03 (Si(CH_3)$_3$), 31.58 (C(CH_3)$_3$), 34.23 (**C**(CH$_3$)$_3$), 119.71, 119.80, 126.04, 127.64, 134.14, 139.74, 141.88, 157.16, 158.86 (Ar). Anal. calc. for $C_{31}H_{45}NO_2Si_2$: C, 71.62; H, 8.72; N, 2.69. Found: C, 71.75; H, 8.80; N, 2.73. HRMS (ESI, m/z): calculated for $C_{31}H_{44}NO_2Si_2H^+$ $[M+H]^+$ *m/z* 520.3062, founded $[M+H]^+$ *m/z* 520.3062.

6,6′-(pyridine-2,6-diyl)bis(4-(t-butyl)-2-(triphenylsilyl)phenol) (5b): This product was prepared as described above for **5a** using **4b** (0.30 g, 0.306 mmol), THF (2 mL), HCl_{conc} (0.32 mL, 3.7 mmol) and stirred over night to give compound **5b** as a light-green powder (m = 0.24 g, 87%, MP 161 °C).

^{1}H NMR ($CDCl_3$, δ, ppm): 1.15 (s., 18H, C(CH_3)$_3$), 7.23 (t., 2H, Ar), 7.25–7.27 (m., 12H, Ar), 7.30 (t., 2H, Ar), 7.32 (t., 3H, Ar), 7.34 (t., 1H, Ar), 7.61 (t., 6H, Ar), 7.63 (t., 6H, Ar), 7.71–7.74 (m., 4H, Ar), 7.91–7.95 (t., 1H, Ar), 10.16 (s., 2H, O**H**). ^{13}C NMR ($CDCl_3$, δ, ppm): 31.32 (C(C**H**)$_3$), 34.12 (**C**(CH)$_3$), 119.93, 120.61, 121.55, 127.63, 129.27, 134.52, 136.32, 137.90, 137.93, 138.85, 142.01, 156.67, 159.17 (Ar). Anal. calc. for $C_{61}H_{57}NO_2Si_2$: C, 82.11; H, 6.44; N, 1.57. Found: C, 82.21; H, 6.50; N, 1.60. HRMS (ESI, m/z): calculated for $C_{61}H_{57}NO_2Si_2H^+$ $[M+H]^+$ *m/z* 892.4001, founded $[M+H]^+$ *m/z* 892.4000.

4.1.2. Synthesis of Complexes 6a and 6b

To a stirred solution of ligand (1 equiv.) in absolute toluene, $AlMe_3$ (1 equiv. of 2.0 M solution in toluene) was added dropwise at −33 °C. The reaction mixture was stirring overnight. After concentration under reduced pressure, the complex was obtained.

For **6a**: starting with **5a** (0.20 g, 0.385 mmol), toluene (4 mL), $AlMe_3$ (0.20 mL, 0.385 mmol). The complex was purified by recrystallization from the toluene/hexane mixture. **6a** was obtained as a light powder (m = 0.18 g, 83%).

^{1}H NMR ($CDCl_3$, δ, ppm): −0.96 (s., 3H, Al-CH_3), 0.33 (s., 18H, Si(CH_3)$_3$), 1.35 (s., 18H, C(CH_3)$_3$), 7.55 (d., 2H, Ar, *J* = 2.51 Hz), 7.60 (d., 2H, Ar, *J* = 2.51 Hz), 7.68 (d., 2H, Ar, *J* = 8.19 Hz), 8.00–8.04 (t., 1H, Ar, *J* = 8.13 Hz). ^{13}C NMR ($CDCl_3$, δ, ppm): −15.72 (Al-CH_3), −0.73 (Si(CH_3)$_3$), 31.58 (C(C**H**)$_3$), 34.20 (**C**(CH)$_3$), 120.16, 120.77, 126.35, 132.23, 136.45, 141.19, 141.35, 155.46, 160.87 (Ar). Anal. calc for $C_{32}H_{46}AlNO_2Si_2$: C, 68.65; H, 8.28; N, 2.50. Found: C, 68.88; H, 8.35; N, 2.45. HRMS (ESI, m/z): calculated for $C_{32}H_{46}AlNO_2Si_2$: $[M+H]^+$ *m/z* 560.2955, founded $[M+H]^+$ *m/z* 560.2947.

For **6b**: starting with **5b** (0.50 g, 0.56 mmol), toluene (5.6 mL), $AlMe_3$ (0.30 mL, 0.56 mmol). The complex was purified by recrystallization from the toluene. **6b** was obtained as a white powder (m = 0.39 g, 76%).

^{1}H NMR ($CDCl_3$, δ, ppm): -1.71 (s., 3H, Al-CH_3), 1.20 (s., 18H, C(CH_3)$_3$), 7.18–7.23 (m., 13H, Ar), 7.31–7.35 (m., 6H, Ar), 7.43–7.44 (d., 2H, Ar, *J* = 2.51 Hz), 7.57–7.60 (m., 13H, Ar), 7.65–7.66 (d., 2H, Ar, *J* = 2.51 Hz), 7.85–7.89 (t., 1H, Ar, *J* = 8.19 Hz). ^{13}C NMR ($CDCl_3$, δ, ppm): -15.80 (Al-CH_3), 31.39 (C(C**H**)$_3$), 34.11 (**C**(CH)$_3$), 120.08, 120.63, 126.35, 127.13, 127.50, 128.22, 129.02, 135.04, 136.50, 139.97, 140.77, 154.88, 161.95 (Ar). Anal. calc. for $C_{62}H_{58}AlNO_2Si_2$: C, 79.88; H, 6.27; N, 1.50. Found: C, 80.01; H, 6.34; N, 1.47. HRMS (ESI, m/z): calculated for $C_{62}H_{58}AlNO_2Si_2$: $[M+Na]^+$ *m/z* 954.3714, founded $[M+Na]^+$ *m/z* 954.3713.

4.1.3. Typical Polymerization Procedure in Bulk

All manipulations were carried out under argon atmosphere. In a 50 mL Schlenk flask, to the initiator (1 equiv) CL or LA (100 or 2000 equiv) was added. Then BnOH (1 equiv) was added with stirring and the reaction mixture was stirred at required temperature (heating was performed with oil bath). The reaction was terminated by the addition of MeOH (1.0 mL), evaporated and purified by reprecipita-

tion using CH_2Cl_2 as a solvent and methanol as a nonsolvent. The polymer was dried in a vacuum at 1 mbar for 3 h.

4.1.4. Typical Polymerization Procedure in Solution

All manipulations were carried out under argon atmosphere. In a 50 ml Schlenk flask, toluene was added to the initiator (1 equiv) (to obtain a 1 M monomer solution). Then, BnOH (1 equiv) and CL or LA (50 or 100 equiv) were added to the resulting solution. The reaction mixture was stirred at the required temperature (heating was performed with oil bath). The reaction was terminated by the addition of MeOH (1.0 mL), evaporated and purified by reprecipitation using CH_2Cl_2 as a solvent and methanol as a nonsolvent. The polymer was dried in a vacuum at 1 mbar for 3 h.

4.1.5. Single Crystal X-ray Diffraction Studies

X-ray diffraction data was collected using Bruker D8 QUEST single-crystal X-ray diffractometer equipped with PHOTONII detector, charge-integrating pixel array detector (CPAD), laterally graded multilayer (Goebel) mirror and microfocus Mo-target X-ray tube (λ = 0.73,071 Å). Data reduction and integration were performed with the Bruker software package SAINT and corrected for absorption and decay by SADABS.[29] Structure was solved by direct methods using SHELXT[30] and refined against F^2 using SHELXL-2018. At 110 K crystal of **6a** ($C_{32}H_{46}AlNO_2Si_2$), M = 559.86, monoclinic, space group $P2_1/n$, Z = 4, a = 10.8708(13), b = 19.529(3) and c = 17.083(2) Å, β = 91.406(4) °, V = 3625.5(8) Å^3. A total of 25,163 (2θmax = 50°) reflections were collected and 6370independent reflections were used for the structure solution and refinement, which converged to R1 = 0.0775 (for 3805 observed reflections), wR2 = 0.1241, GOF = 1.144. At 100 K crystal of **6b** ($C_{62}H_{58}AlNO_2Si_2$, C_7H_8), M = 1024.38, monoclinic, space group $P2_1/c$, Z = 4, a = 10.927(2), b = 20.833(4) and c = 25.080(5) Å, β = 94.38(3)°, V = 5692(2) Å^3. A total of 34,931 (2θmax = 50°) reflections were collected and 9997 independent reflections were used for the structure solution and refinement, which converged to $R1$ = 0.0750 (for 5769 observed reflections), w$R2$ = 0.2248, GOF = 1.004.

CCDC 2,374,530 (**6a**) and CCDC 2,389,000 (6**b**) contains the supplementary crystallographic data for this paper. These data can be obtained free of charge from The Cambridge Crystallographic Data Centre via http://www.ccdc.cam.ac.uk.

Acknowledgements

This work was supported by the Russian Science Foundation (grant no. 20-13-00391). The study of the structure of compounds **6a** and **6b** by X-ray diffraction analysis (K.A.L.) and the molecular weight characteristics of polymers (E.V.Ch.) were funded by the Moscow University Development Program. The study of aluminum complex was carried out on an Agilent 400-MR NMR spectrometer (the Moscow University Development Program), X-ray diffraction studies were carried out using the "X-ray diffractometer for the analysis of single crystals Bruker D8 QUEST" (the Moscow University Development Program), the molecular weights of the polymers were determined on a multi-detector GPC/SEC system (the Moscow University Development Program). Experimental TG-DSC-DTG studies were carried out on facilities at the "Nanochemistry and Nanomaterials" Center for Collective Use, Department of Chemistry, M. V. Lomonosov Moscow State University.

Conflict of Interests

The authors declare no conflict of interest.

Data Availability Statement

The data that support the findings of this study are available in the Supporting Information of this article.

Keywords: Aluminum · Biodegradable polymers · Lactide · Metal complexes · Ring-opening polymerization · E-caprolactone

[1] H. R. Kricheldorf, S. M. Weidner, *Polym. Chem.* **2022**, *13*, 1618.
[2] T. Fuoco, D. Pappalardo, *Catalysts* **2017**, *7*, 64.
[3] a) J. Gao, D. Zhu, W. Zhang, G. A. Solan, Y. Ma, W.-H. Sun, *Inorg. Chem. Front.* **2019**, *6*, 2619; b) B. N. Mankaev, S. S. Karlov, *Materials* **2023**, *16*, 6682.
[4] a) A. Le Borgne, V. Vincens, M. Jouglard, N. Spassky, *Makromolekulare Chemie. Macromolecular Symposia* **1993**, *73*, 37; b) N. Spassky, M. Wisniewski, C. Pluta, A. L.e Borgne, *Macromol. Chem. Phys.* **1996**, *197*, 2627; c) C. P. Radano, G. L. Baker, M. R. Smith, *J. Am. Chem. Soc.* **2000**, *122*, 1552; d) T. M. Ovitt, G. W. Coates, *J. Am. Chem. Soc.* **2002**, *124*, 1316; e) B. Gao, R. Duan, X. Pang, X. Li, Z. Qu, Z. Tang, X. Zhuang, X. Chen, *Organometallics* **2013**, *32*, 5435; f) Z. Zhong, P. J. Dijkstra, J. Feijen, *Angew. Chem. Int. Ed.* **2002**, *41*, 4510; g) N. Nomura, R. Ishii, Y. Yamamoto, T. Kondo, *Chem. – Europ. J.* **2007**, *13*, 4433; h) N. Maudoux, T. Roisnel, V. Dorcet, J.-F. Carpentier, Y. Sarazin, *Chem. – Europ. J.* **2014**, *20*, 6131; i) Z. Guo, R. Duan, M. Deng, X. Pang, C. Hu, X. Chen, *Sci. China: Chem.* **2015**, *58*, 1741; j) Z. Wen, D. Li, J. Qi, X. Chen, Y. Jiang, L. Chen, B. Gao, Y. Cui, Q. Duan, *Colloid. Polym. Sci.* **2015**, *293*, 3449; k) W. Luo, T. Shi, S. Liu, W. Zuo, Z. Li, *Organometallics* **2017**, *36*, 1736; l) C. Kan, J. Ge, H. Ma, *Dalton Trans.* **2016**, *45*, 6682; m) M. Strianese, D. Pappalardo, M. Mazzeo, M. Lamberti, C. Pellecchia, *Dalton Trans.* **2020**, *49*, 16533.
[5] a) E. A. Kuchuk, K. V. Zaitsev, F. A. Mamedova, A. V. Churakov, G. S. Zaitseva, D. A. Lemenovsky, S. S. Karlov, *Russ. Chem. Bull.* **2016**, *65*, 1743; b) C.-T. Chen, C.-A. Huang, B.-H. Huang, *Macromolecules* **2004**, *37*, 7968; c) C.-T. Chen, C.-A. Huang, B.-H. Huang, *Dalton Trans.* **2003**, *19*, 3799; d) E. D. Cross, G. K. Tennekone, A. Decken, M. P. Shaver, **2013**, *1*, 79; e) L. C. Liang, S. T. Lin, C. C. Chien, *J. Chin. Chem. Soc.* **2013**, *60*, 710; f) Z. Tang, V. C. Gibson, *Eur. Polym. J.* **2007**, *43*, 150.
[6] a) I. Nifant'ev, P. Ivchenko, *Molecules* **2019**, *24*, 4117; b) I. Nifant'ev, P. Ivchenko, *Polymers* **2019**, *11*, 2078.
[7] a) W. Meelua, M. Linnolahti, J. Jitonnom, *RSC Adv.* **2024**, *14*, 11715; b) M. C. D'Alterio, S. Moccia, Y. Rusconi, C. De Rosa, G. Talarico, *Catal. Sci. Technol.* **2024**, *14*, 5624; c) Y. Rusconi, M. C. D'Alterio, C. De Rosa, Y. Lu, S. M. Severson, G. W. Coates, G. Talarico, *ACS Catal.* **2024**, *14*, 318; d) Y. Rusconi, M. C. D'Alterio, A. Grillo, A. Poater, C. De Rosa, G. Talarico, *Polymer* **2024**, *292*, 126639.
[8] a) Y.-L. Hsieh, W. Benchaphanthawee, H.-H. Teng, N. Huang, J.-H. Yang, J.-R. Sun, G.-H. Lee, N. Kungwan, C.-H. Peng, *Polymer* **2023**, *267*, 125687; b) D. Chandanabodhi, T. Nanok, *Mol. Catal.* **2017**, *436*, 145; c) I. Nifant'ev, A. Shlyakhtin, M. Kosarev, D. Gavrilov, S. Karchevsky, P. Ivchenko, *Polymers* **2019**, *11*, 1641; d) I. Nifant'ev, P. Komarov, V. Ovchinnikova, A. Kiselev, M. Minyaev, P. Ivchenko, *Polymers* **2020**, *12*, 2273; e) L. Wang, C. E. Kefalidis, S. Sinbandhit, V. Dorcet, J.-F. Carpentier, L. Maron, Y. Sarazin, *Chem. - Eur. J.* **2013**, *19*, 13463; f) M. V. Zabalov, B. N. Mankaev, M. P. Egorov, S. S. Karlov, *Int. J. Mol. Sci.* **2022**, *23*, 15523; g) M. V. Zabalov, B. N. Mankaev, M. P. Egorov, S. S. Karlov, *Russ. Chem. Bull.* **2023**, *72*, 602; h) Y. Wongnongwa, S. Haesuwannakij, K. Udomsasporn, P. Chumsaeng, A. Watcharapasorn, K. Phomphrai, S. Jungsuttiwong, *Polymer* **2023**, *281*, 126065.
[9] M. Mandal, A. M. Luke, B. Dereli, C. E. Elwell, T. M. Reineke, W. B. Tolman, C. J. Cramer, *ACS Catal.* **2019**, *9*, 885.
[10] a) J. S. Klitzke, T. Roisnel, E. Kirillov, O. d. L. Casagrande Jr., J.-F. Carpentier, *Organometallics* **2014**, *33*, 309; b) J. S. Klitzke, T. Roisnel, E.

Kirillov, O. d. L. Casagrande Jr., J.-F. Carpentier, *Organometallics* **2014**, *33*, 5693; c) B. N. Mankaev, V. A. Serova, M. U. Agaeva, K. A. Lyssenko, A. N. Fakhrutdinov, A. V. Churakov, E. V. Chernikova, M. P. Egorov, S. S. Karlov, *J. Organomet. Chem.* **2024**, *1005*, 122973.
[11] T. Agapie, J. E. Bercaw, *Organometallics* **2007**, *26*, 2957.
[12] L. Yang, D. R. Powell, R. P. Houser, *Dalton Trans.* **2007**, *9*, 955.
[13] B. N. Mankaev, L. F. Hasanova, A. V. Churakov, M. P. Egorov, S. S. Karlov, *Int. J. Mol. Sci.* **2022**, *23*, 15649.
[14] a) H. Ma, J. Okuda, *Macromolecules* **2005**, *38*, 2665; b) N. Spassky, V. Simic, M. S. Montaudo, L. G. Hubert-Pfalzgraf, *Macromol. Chem. Phys.* **2000**, *201*, 2432; c) W. A. Munzeiwa, B. Omondi, V. O. Nyamori, *Polyhedron* **2017**, *138*, 295.
[15] a) M. Bouyahyi, E. Grunova, N. Marquet, E. Kirillov„ C. M. Thomas, T. Roisnel, J.-F. Carpentier, *Organometallics* **2008**, *27*, 5815; b) A. Kowalski, A. Duda, S. Penczek, *Macromolecules* **1998**, *31*, 2114; c) M. Save, M. Schappacher, A. Soum, *Macromol. Chem. Phys.* **2002**, *203*, 889.
[16] B. M. Chamberlain, M. Cheng, D. R. Moore, T. M. Ovitt, E. B. Lobkovsky, G. W. Coates, *J. Am. Chem. Soc.* **2001**, *123*, 3229.
[17] C. Sattayanon, W. Sontising, J. Jitonnom, P. Meepowpan, W. Punyodom, N. Kungwan, *Comput. Theor. Chem.* **2014**, *1044*, 29;
[18] A. V. Marenich, C. J. Cramer, D. G. Truhlar„ *J. Phys. Chem. B* **2009**, *113*, 6378.
[19] a) J. P. Perdew, K. Burke, M. Ernzerhof, *Phys. Rev. Lett.* **1996**, *77*, 3865; b) M. Ernzerhof, G. E. Scuseria, *J. Chem. Phys.* **1999**, *110*, 5029.
[20] a) D. N. Laikov, *Chem. Phys. Lett.* **1997**, *281*, 151; b) D. N. Laikov, Y. A. Ustynyuk, *Russ. Chem. Bull.* **2005**, *54*, 820.
[21] a) E. Caldeweyher, C. Bannwarth, S. Grimme, *J. Chem. Phys.* **2017**, *147*, 034112; b) E. Caldeweyher, S. Ehlert, A. Hansen, H. Neugebauer, S. Spicher, C. Bannwarth, S. Grimme, *J. Chem. Phys.* **2019**, *150*, 154122; c) E. Caldeweyher, J.-M. Mewes, S. Ehlert, S. Grimme, *Phys. Chem. Chem. Phys.* **2020**, *22*, 8499.
[22] a) E. R. Johnson, S. Keinan, P. Mori-S´anchez, J. Contreras-Garcia, A. J. Cohen, W. Yang, *J. Am. Chem. Soc.* **2010**, *132*, 6498; b) R. Laplaza, F. Peccati, R. A. Boto, C. Quan, A. Carbone, J.-P. Piquemal, Y. Maday, J. Contreras-Garcia, *Wiley Interdiscip. Rev.: Comput. Mol. Sci.* **2021**, *11*, e1497; c) T. Novoa, R. Laplaza, F. Peccati, F. Fuster, J. Contreras-Garcia, *J. Chem. Inf. Model.* **2023**, *63*, 4483.
[23] J. Contreras-Garcia, E. R. Johnson, S. Keinan, R. Chaudret, J.-P. Piquemal, D. N. Beratan, W. Yang, *J. Chem. Theory Comput.* **2011**, *7*, 625.
[24] a) F. Neese, *WIREs Comput. Mol. Sci.* **2012**, *2*, 73; b) F. Neese, *WIREs Comput. Mol. Sci.* **2018**, *8*, e1327; c) F. Neese, *WIREs Comput. Mol. Sci.* **2022**, *12*, e1606.
[25] F. Weigend, R. Ahlrichs, *Phys. Chem. Chem. Phys.* **2005**, *7*, 3297.
[26] a) E. W. Lewis, *J. Chem. Soc. Transactions* **1903**, *83*, 329; b) A. Podgoršek, S. Stavber, M. Zupan, J. Iskra, *Tetrahedron* **2009**, *65*, 4429.
[27] C. Marvel, P. Porter, *J. Organic Synth.* **1941**, *1*, 377.
[28] C. H. Low, J. N. Rosenberg, M. A. Lopez, T. Agapie, *J. Am. Chem. Soc.* **2018**, *140*, 11906.
[29] L. Krause, R. Herbst-Irmer, G. M. Sheldrick, D. Stalke, *J. Appl. Crystallogr.* **2015**, *48*, 3.
[30] G. Sheldrick, *Acta Cryst* **2015**, *71*, 3.

Manuscript received: September 06, 2024